

Journal of Materials Chemistry A

Accepted Manuscript



This is an *Accepted Manuscript*, which has been through the Royal Society of Chemistry peer review process and has been accepted for publication.

Accepted Manuscripts are published online shortly after acceptance, before technical editing, formatting and proof reading. Using this free service, authors can make their results available to the community, in citable form, before we publish the edited article. We will replace this *Accepted Manuscript* with the edited and formatted *Advance Article* as soon as it is available.

You can find more information about *Accepted Manuscripts* in the [Information for Authors](#).

Please note that technical editing may introduce minor changes to the text and/or graphics, which may alter content. The journal's standard [Terms & Conditions](#) and the [Ethical guidelines](#) still apply. In no event shall the Royal Society of Chemistry be held responsible for any errors or omissions in this *Accepted Manuscript* or any consequences arising from the use of any information it contains.



Soluble Salt Self-Assembly-Assisted Synthesis of Three-Dimensional Hierarchical Porous Carbon Networks for Supercapacitors †

Received 00th January 20xx,
Accepted 00th January 20xx

DOI: 10.1039/x0xx00000x

www.rsc.org/

Shan Zhu ^a, Jiajun Li ^a, Chunnian He ^{a,b,*}, Naiqin Zhao ^{a,b,*}, Enzuo Liu ^{a,b}, Chunsheng Shi ^a, Miao Zhang ^a

Three-dimensional (3D) hierarchical porous carbons (indicated with 3D HPCs) were synthesized via a simple one-pot method using the self-assembly of various water-soluble NaX salts (X: Cl⁻, CO₃²⁻, SiO₃²⁻) as a structure-directing template. By controlling crystallization and assembly of multi-scale salts via freeze-drying processing, 3D porous carbon networks with tailored pore size distribution have been generated by calcining the salts/glucose self-assembly followed by removing the 3D self-assembly of NaX salts via simple water washing. When evaluated their applications for supercapacitor electrodes as an example, the as-constructed 3D HPCs with large surface area, high electron conductivity, facile electrolyte penetration and robust structure exhibited excellent capacitive performance, namely, high specific capacitance (320 F g⁻¹ at 0.5 A g⁻¹), outstanding high rate capacitance retention (126 F g⁻¹ at 200 A g⁻¹), and superior specific capacitance retention ability (nearly no discharge capacity decay between 1000 and 10 000 continuous charge–discharge cycles at a high current density of 5 A g⁻¹). Based on our soluble salt self-assembly-assisted synthesis concept, it was revealed that salts in the seawater are also very suitable for low-cost and scalable synthesis of 3D HPCs with good capacitive performance, which pave the way for advanced utilization of seawater.

Introduction

Owing to their well-developed porosity, high surface area, excellent electric conductivity and thermal conductivity coupled with light weight and chemical stability, porous carbon materials are of great interest for a variety of energy-based applications, such as supercapacitor, lithium ion battery and fuel cell.^{1–7} However, conventional porous carbon materials, which are usually prepared by high-temperature pyrolysis followed by a physical or chemical activation process, have broad pore-size distributions mostly in the micropores (< 2 nm) range with little control.⁸ Although it can obtain high specific surface area (SSA), the microporous structure which is too narrow to transfer mass efficiently, suffers from critical drawbacks in transport kinetics, thus limiting their application range. In this regards, a lot of efforts have been invested in the development of hierarchical porous carbons (HPCs) that can integrate the merits of various length scales of pores including micropores (<2 nm), mesopores (2~50 nm), and macropores

(>50 nm).⁸ In general, the macropores are favorable for the mass transport; mesopores enhance the interface contact, which is especially important for electrolyte-based applications; while the micropores increase the SSA and introduce the reactive active sites.^{9,10}

Recently, numerous HPCs with well-developed hierarchical porous structures have been developed via template replication methods. Among those, inorganic templates such as zeolites,¹¹ ordered mesoporous silica (OMS),¹² colloidal silicas,¹³ and polymer beads¹⁴ have been widely employed to create meso/macropores constructed carbon framework, while soft templates including ionic surfactants and non-ionic amphiphilic block copolymers have been utilized for the direct synthesis of ordered mesopores on macro-structured carbon matrix.^{15–17} However, the former technique requires application of highly corrosive toxic or even toxic reagents, such as KOH or HF,^{18,19} for the removal of hard templates; the latter is restricted to low temperature treatment. Moreover, both of two methods are very costly, time and energy consuming due to the tedious preparation of templates in advance. In order to overcome above issues, Fechner and co-workers²⁰ have developed a simple and sustainable pathway, i.e. in situ salt templating strategy, toward porous carbons with high surface areas. Unfortunately, the as-made porous carbons exhibit disorder morphology, and their pore size distribution, which is largely limited to micro- and mesoporous, is very hard to be tailored.

^a School of Materials Science and Engineering and Tianjin Key Laboratory of Composites and Functional Materials, Tianjin University, Tianjin 300072, China. Email: cnhe08@tju.edu.cn nqzhao@tju.edu.cn

^b Collaborative Innovation Center of Chemical Science and Engineering, Tianjin 300072, China

† Electronic Supplementary Information (ESI) available: SEM, TEM, XPS, XRD and Electrochemical Test. See DOI: 10.1039/x0xx00000x

In this work, we demonstrated a facile and scalable one-pot approach using the 3D assembly of various NaX salts (X: Cl⁻, CO₃²⁻, SiO₃²⁻) as a template system for the synthesis of HPCs, which not only possess 3D ordered network structure, also have pores that can be tuned in a wide range. By controlling the content and crystallization of salts during freeze-drying processing, multi-scale salts were self-assembled into 3D structure. After carbonization and simple water washing, the carbon precursors homogeneously coated on the surface 3D assembly of multi-scale salt template system were converted into 3D porous carbon network with controllable hierarchical pores and surface area. When utilized as the electrode of the supercapacitors, the 3D HPCs with large surface area and high electron conductivity exhibited superior charge storage capacity and great rate stability. Furthermore, this unique strategy can be extended to sea salts as the soluble templates for the synthesis of 3D HPCs, being benefit in extremely low-cost, green, and scaled up production.

Experimental

Synthesis of 3D HPCs

During the synthesis, various soluble salts with different sizes serve as templates for fabricating 3D HPCs. According to the template sizes, the corresponding pores are labeled as -B, -M, -S, meaning to Big, Medium, and Small, respectively. For preparing 3D HPC-BMS, glucose (1.25 g), NaCl (20 g), Na₂CO₃ (0.5 g) and Na₂SiO₃ (0.5 g) were dissolved in 75 ml of deionized water. The resulting mixed solution was frozen in -10 °C and freeze-dried at -55 °C in vacuum and then grounded by agate mortar to obtain very fine composite powder (~100 mesh). The model of vacuum freeze drying machine is FD-1-50 (Beijing Bicol Scientific Instruments Co., Ltd.). After that, the composite powders were heated at 650 °C for 2 h in a tube furnace under flowing Ar atmosphere (200 ml min⁻¹). Once cooled to room temperature, the obtained powders were washed with deionized water to dissolve salts and then pure 3D HPC-BMS was obtained. For comparison, HPC-B, -M, -S, -BM, -MS, -BS were also synthesized at the same conditions as those for producing HPC-BMS, with the raw materials listed in Table S1. Moreover, the carbon bulk (CB) was also prepared by using the same method without the salts.

Synthesis of porous carbon using salts from seawater

Firstly, the raw seawater (750 ml, obtained from Bohai Sea) is filtered to remove the insoluble substances, and evaporated part of water (around 85% of total mass). Then glucose (1.25 g) is dissolved in the concentrated seawater. After that, the mixture was treated with the same conditions as that of HPC-B to obtain the final product of porous carbon (denoted with HPC-sw).

Material characterization

Transmission electron microscope (TEM), high-resolution TEM (HRTEM) and scanning TEM (STEM) were performed on a FEI Tecnai G² F20 TEM. Scanning electronic microscopy (SEM) images were carried out by Hitachi S4800. X-ray

diffraction (XRD) measurements were taken on a Rigaku D/max diffractometer with Cu K α radiation. Brunauer-Emmett-Teller (BET) surface areas and porosities of the products were determined by nitrogen adsorption and desorption using a Micromeritics ASAP 2020 analyzer. The micropores surface areas are calculated by the t-plot method. X-ray photoelectron spectroscopy (XPS) was carried out on PHI5000VersaProbe. Raman spectrum was conducted on the LabRAM HR Raman spectrometer by applying Ar ion laser source at the laser excitation of 514.5 nm.

Electrochemical measurements

The electrochemical performance of the 3D HPC electrode was analyzed using a cell with a three-electrode configuration in 6 M KOH electrolyte. The working electrodes were made through the following steps: active materials, conductivity agent (carbon black), and binder (polytetrafluoroethylene, PTFE) in a weight ratio of 80:10:10 were blended with ethanol as solvent. Electrode film prepared by coating the mixture on nickel foam was first vacuum-dried at 80 °C overnight and then pressured at 8 MPa for 3 min. The loading mass of active materials on each current collector was 1.0~2.0 mg, and area was 0.81 cm². For two electrodes system, two identical (by weight and size) electrodes were separated by an ion porous separator (Whatman, Filter paper) soaked with electrolyte, then assembled as a Coin cells (CR2032). All of electrochemical performances tests were conducted on a CHI660D electrochemical workstation. The specific capacitances Cs in this paper are calculated from galvanostatic charge/discharge curves according to $C_s = It/m \Delta V$, where I is the charge/discharge current, t the discharge time, and ΔV the voltage difference.

Results and discussion

The synthesis of 3D HPC-BMS involves self-assembly of multi-scale soluble salts (NaCl, Na₂CO₃ and Na₂SiO₃) coated with carbon precursor (glucose) via freeze-drying processing, and carbonization of glucose followed by water-washing, as schematically elucidated in Fig. 1. First of all, glucose and three kinds of NaX salts (X: Cl⁻, CO₃²⁻, SiO₃²⁻) were dissolved in distilled water to get a homogeneous solution. Secondly, a freeze-drying treatment was carried out on the homogeneous solution to remove water. At this stage, the salts were crystallized to form multi-scale (from nanometers to

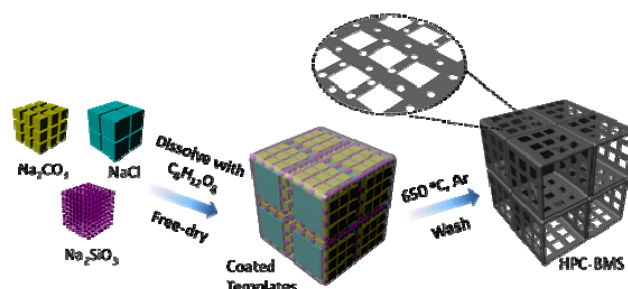


Fig. 1. Schematics demonstrating the fabrication process of 3D HPC-BMS with the assistance of multi-scale soluble salt self-assembly.

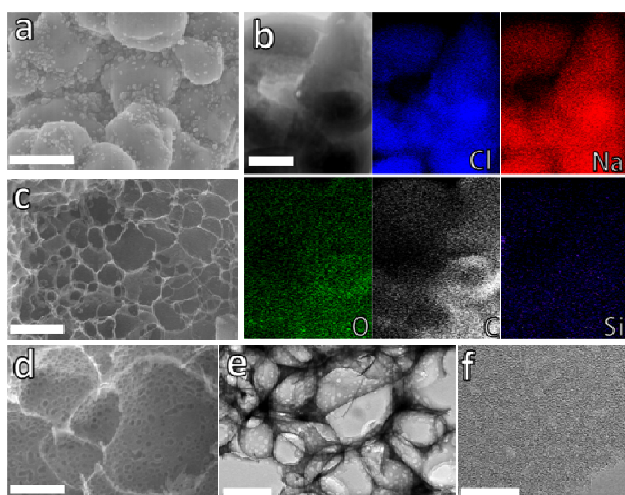


Fig. 2. (a) SEM image of NaCl-Na₂CO₃-Na₂SiO₃ assembly coated by carbon before water washing. (b) STEM image and element mappings, exhibiting the distribution of Na, Cl, C, O, Si. (c, d) SEM images, (e) TEM and (f) HRTEM images of HPC-BMS. The scale bars: (a, b, c, e) 1 μ m, (d) 500 nm, (f) 10 nm.

micrometers) salt particles. Meanwhile, the multi-scale salt particles evenly coated with glucose were self-assembled into 3D structure. Upon heating the 3D structure at 650 $^{\circ}$ C under Ar, the glucose was carbonized to generate carbon coating around the surface of multi-scale salt self-assembly. Finally, the as-obtained solid powders were treated with distilled water to remove salts and thus pure 3D HPCs (HPC-BMS) were obtained.

The calcined products before removing salts were characterized by SEM. From Fig. 2a and Fig. S1, it can be observed that salt particles with different sizes were assembled into 3D architecture, which was coated by carbon layer evenly, indicating that this 3D hierarchical assembly structure was maintained during the heat treatment process and thus served as templates for fabricating 3D HPC-BMS. Furthermore, STEM and elements mapping (Fig. 2b) were performed to determine the detailed distribution of these salt particles. It is clearly seen that the micrometer-sized cubic NaCl particles assembled together, whose surfaces were homogeneously dispersed with Na₂CO₃ and Na₂SiO₃ particles. Such combination of salts with different length scales not only ensures the densely stacking of templates for enhancing filling of carbon precursor, but also results in a hierarchical structure of final product for improving the electrochemical properties.^{1,4,20-22}

After removing the templates by simply water washing, the as-obtained 3D HPC-BMS were investigated by SEM, TEM

and HRTEM. As seen from SEM image in Fig. 2c, the architecture of HPC-BMS exhibits a typical 3D porous network with micrometer-sized macropores, which is an assembly of fully and orderly interconnected ultrathin carbon nanosheets. The magnified SEM image of Fig. 2d demonstrates a mass of mesopores ranging from 50 to 100 nm in the carbon nanosheet network walls, and the network walls display obvious corrugations, indicating that the network walls have excellent mechanical flexibility. The interconnected 3D HPC-BMS network was further validated by TEM. As shown in Fig. 2e, a continuous 3D porous network is observed. In addition, it can be seen clearly numerous mesopores in the network walls, in good agreement with above SEM results. HRTEM image (Fig. 2f) of the carbon nanosheet wall further substantiated that the carbon nanosheet walls also have abundant and uniform nanopores of about 5 nm in their structure. Above results showed that the as-obtained 3D HPC-BMS indeed possesses hierarchical porous structure including macropores (1–2 μ m), mesopores (50–100 nm) and nanopores (\sim 5 nm). This structure is very suitable for energy storage. When the interconnected 3D HPC-BMS networks are immersed in the electrolyte, a great deal of the electrolyte is initially stored in the interconnected ion-buffering reservoirs and, meanwhile, the extreme thin carbon nanosheet walls around them are covered by it, providing a quick supply and short diffusion distance.

It should be noted that without the assistance of salt template, only bulk-like carbon material (CB) were obtained by the same synthesis method (see Fig. S2), indicating that the salt templates have great influence on the formation of 3D HPCs. In order to unveil the effect of the three kinds of salt template adopted on the synthesis of 3D HPCs, a series of contrast experiments based on single and dual templates were conducted, whose preparation details are described in experiment section. When using single salt template during the preparation process, it was found that only porous carbon networks with single pore size distribution were produced (as shown in Fig. S3). For instance, 3D porous carbon network with the pore size of 1–2 μ m,²¹ 3D porous carbon network with the pore size of 50–100 nm was derived from the assembly of Na₂CO₃ particles (50–100 nm), while porous carbon network with the pore size of around 5–10 nm was achieved due to Na₂SiO₃ (5–10 nm) assembly template. Besides, the abundant micropores resulted from the pyrolysis of glucose (Fig. S4). As for the utilization of dual templates during the synthesis of 3D HPCs, interestingly, porous carbon networks with dual pore size distributions were

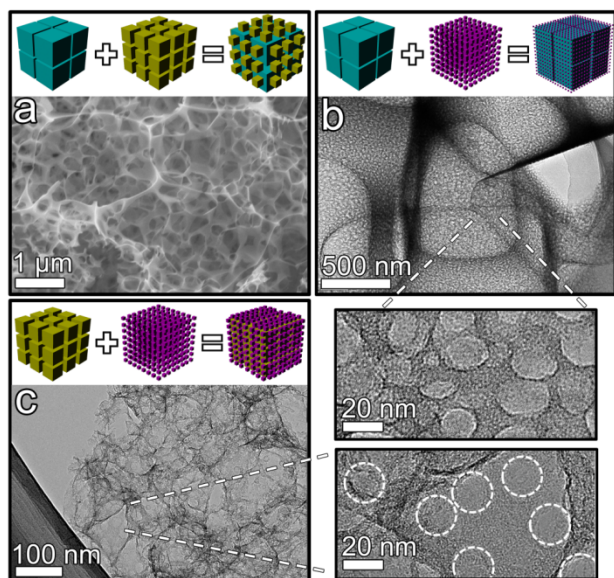


Fig. 3. Morphology demonstration of hierarchical carbon structures produced with the assistance of multiple-sized salt templates. (a) SEM image of HPC-BM; TEM images of (b) HPC-BS, (c) HPC-MS, and the partial enlarged Figs belong to HPC-BS and HPC-MS respectively.

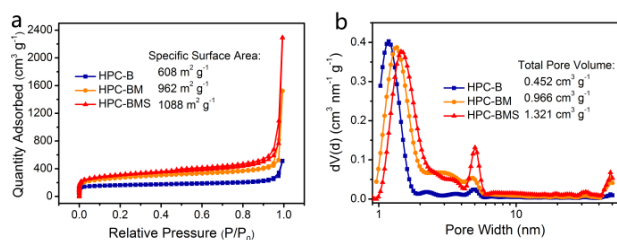


Fig. 4. (a) Adsorption-desorption isotherms and (b) pore size distributions of HPC-B, HPC-BM and HPC-BMS.

obtained (as shown in Fig. 3). Taken HPC-BS as an example, we firstly mixed NaCl and Na_2SiO_3 with carbon source. After freeze-drying and heat treatment process, the NaCl particles with 1–2 μm were assembled into a 3D architecture (Fig. S5a), while the small Na_2SiO_3 particles (5–10 nm) were evenly dispersed on the surface of big NaCl particles (see Fig. S5b). After the simple water washing to remove the templates, the as-obtained carbon network exhibits a typical 3D hierarchical architecture, in which the mesopores derived from Na_2SiO_3 are densely distributed on the walls of macropores (Fig. 3b), well consistent with the pore size distribution analysis (Fig. S6). Therefore, keeping the features of the macropores caused by NaCl, Na_2SiO_3 particles were successfully introduced as the template of the second order of porosity. As shown in Fig. 3, the HPC-BM and HPC-MS also have the same phenomena, indicating the general concept of salt self-assembly template system during the synthesis process of HPC: these templates with various scales are compatible with each other and can be used as “module unit” to build numerous hierarchical structures with controlled morphology and properties.

Nitrogen physisorption measurements were carried out at 196 $^\circ\text{C}$ to analyze the textural characteristics of the 3D HPCs obtained by the carbonization of glucose using single salt

template (NaCl), dual salt templates (NaCl and Na_2CO_3) and three salt templates (NaCl, Na_2CO_3 and Na_2SiO_3). The N_2 sorption isotherms and the pore size distributions are shown in Fig. 4a and b, respectively. According to the isotherm profiles displayed in Fig. 4a, the isotherm curve of HPC-B can be categorized as being of type II, indicating that this structure has few mesopores in its pore size distribution. In contrast, the isotherm curves of HPC-BMS as well as HPC-BS and HPC-MS are all ascribed to typical IV and exhibit a hysteresis loop at a relative pressure in the range of 0.40–0.97, suggesting a mesoporous structure and narrow mesopore size distribution. The specific surface area and pore volume of HPC-BMS are calculated to be $1088 \text{ m}^2 \text{g}^{-1}$ and $1.321 \text{ cm}^3 \text{g}^{-1}$ (Table 1), respectively, by the BET analysis, which are much larger than the HPC-B ($608 \text{ m}^2 \text{g}^{-1}$). This indicates that the introduction of nanosized Na_2SiO_3 can remarkably enhance the surface area and pore volume of 3D HPC-BMS. For comparison, without salt templates during the synthesis, the as-obtained CB can only have a low SSA of $19.5 \text{ m}^2 \text{g}^{-1}$ (Fig. S4).

In order to further explore the pore evolution of HPCs based on the utilization of multiple templates, we firstly

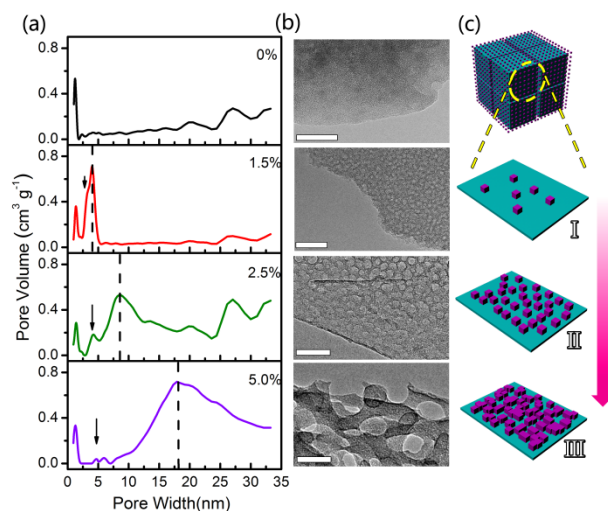


Fig. 5. (a) Pore size distributions and (b) the corresponding TEM images of HPC-BS based on different mass ratio of Na_2SiO_3 to NaCl from 0%, 1.5% to 2.5% and 5%. (The scale bars are 50 nm) (c) Scheme of the morphology evolution of combination templates.

focused on HPC-BS and obtained a series of samples with controllable pores by adjusting the ratio of the two kinds of salts, namely NaCl and Na_2SiO_3 (Fig. 5 and Fig. S7). According to the pore size distributions of Fig. 5a, the average mesopores size rises from 0, 4, 8 to 18 nm (indicated with black dash lines) with increasing the weight ratio of $\text{Na}_2\text{SiO}_3/\text{NaCl}$ from 0, 1.5%, 2.5% to 5%. Well consistent with the pore size distributions, TEM observations (Fig. 5b) further verified the successful regulation of the mesopores size in the BET analysis. The pore evolution process of HPCs derived from such dual templates can be described as follows: initially, NaCl emerges from the solution to form crystal with micrometer-size, and provides a platform for the precipitation of tiny Na_2SiO_3 nanoparticles (4 nm in diameters); then, with the increase of Na_2SiO_3 amount,

more and more Na_2SiO_3 nanoparticles emerged from the solution cover the surface of NaCl particles; when the addition amount of Na_2SiO_3 reaches to a certain degree, the Na_2SiO_3 nanoparticles would aggregate into bigger ones (more than 4 nm) and thus lead to the formation of mesopores with larger pore size. As for the HPC-BM resulted from NaCl - Na_2CO_3 dual template system, their pore also follows this evolution mechanism, and the micropore size of HPC-BM can be tuned from 50 to 200 nm by adjusting the ratio of Na_2CO_3 to NaCl .

Table 1. Physicochemical characterization of HPC-B, HPC-M, HPC-S, HPC-BM, HPC-BS, HPC-MS

Samples	BET surface area [$\text{m}^2 \text{g}^{-1}$]	Total pore volume [$\text{cm}^3 \text{g}^{-1}$]	Micropores surface area [$\text{m}^2 \text{g}^{-1}$]
HPC-B	608	0.452	506
HPC-M	892	0.472	787
HPC-S	588	1.549	382
HPC-BM	962	0.966	723
HPC-BS	692	0.856	440
HPC-MS	850	1.533	386
HPC-BMS	1088	1.321	776

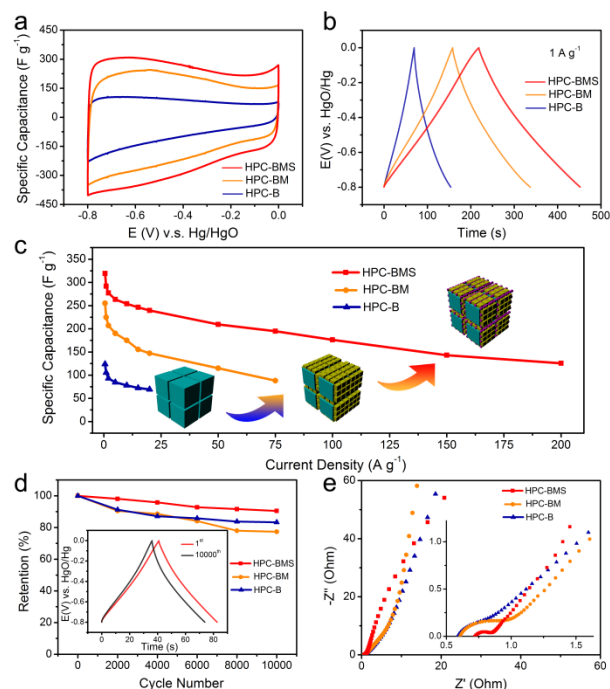


Fig. 6. Electrochemical performance of HPC-B, HPC-BM and HPC-BMS measured in a three-electrode system. (a) CV curves at a scan rate of 5 mV s⁻¹. (b) Charge-discharge profiles at the current density of 1 A g⁻¹. (c) Specific capacitances at different current densities. (d) Long-cycle performance conducted at 5 A g⁻¹, and the insert shows the charge/discharge curves at the 1st and 10000th cycles of HPC-BMS. (e) Electrochemical impedance spectra of HPC-B, HPC-BM and HPC-BMS.

On the basis of above evidences, the surface area and porous structure of 3D HPCs can be facily tuned by using different salt templates. When integrating the templates of NaCl , Na_2CO_3 and Na_2SiO_3 , the as-prepared 3D HPC-BMS shows high surface area and excellent hierarchical porous structure, which are very favorable for the mass transport of electrolyte and thus

present promising materials in the fields of catalyst, sensor and energy storage and conversion, etc.²³

The characteristic of the carbon in the 3D HPC-BMS were further evaluated using Raman spectroscopy. The spectrum of Fig. S8 obviously reveals the presence of D band at 1338 cm⁻¹, and G band at 1593 cm⁻¹. It is well-known that the D band is ascribed to the vibrations of carbon atoms with dangling bonds for the in-plane terminations of disordered graphite, while the G band is the result of the E_{2g} mode (stretching vibrations) in the basal plane of the crystalline graphite. In general, the integral intensity ratio of D peak to G peak (I_D/I_G) is used to evaluate the crystallization degree of carbon materials. The value of I_D/I_G of our HPC-BMS is 0.79, demonstrating that the carbon networks are partially graphitized.²⁴ XRD pattern of Fig. S9 displays two broad diffraction peaks at $2\theta = 26^\circ$ and 42° , corresponding to the (002) and (100) reflections of graphite, respectively.²⁵ XPS analysis of HPC-BMS (Fig. S10) reveals the existence of 6 at.% oxygen atoms induced by the pyrolysis of glucose, which will give rise to many kinds of functional group (such as C=O and C-O-C) and introduce pseudocapacitance to enhance the capacitive performance.²²

3D hierarchical porous carbon materials (e.g. activated carbon,²⁶ carbide-derived carbon²⁷ and templated carbon³) have been extensively studied in the field of energy storage due to their high surface areas and rich porous pore structures. One of the most promising energy storage application is supercapacitor, which stores charge in electrochemical double layers.^{3,28} In this regards, we investigated the capacitive properties of 3D HPCs in a three-electrode system by using 6 M KOH as the electrolyte. When tested at a scan rate of 5 mV s⁻¹, all samples (HPC-B, HPC-BM and HPC-BMS) present the rectangle-like shape of CV curves (as shown in Fig. 6a), implying an electric double layer capacitive mechanism.²⁸ Combined with CV, the symmetric of the galvanostatic charge/discharge profiles at 1 A g⁻¹ reveals the typical capacitive behaviour of these carbon networks (Fig. 6b).

Since the electric double layer capacitor is a surface phenomenon, a larger surface area is very beneficial for achieving a higher capacitance. Compared with HPC-B, HPC-M, HPC-S, HPC-BM, HPC-BS, HPC-MS, the HPC-BMS delivered much superior performance (as compared in Fig. 6c, Fig. S11, S12, S13 and S14): the calculated capacitance of HPC-BMS based on discharge results is 320 F g⁻¹ at 0.5 A g⁻¹ (Fig. 6c). When tested at 20 A g⁻¹, the capacitance of HPC-BMS performs 240 F g⁻¹. In contrast, HPC-BM and HPC-B can only carry out 69 and 147 F g⁻¹, respectively. Even tested at 200 A g⁻¹, an extremely high current density, the specific capacitance of HPC-BMS can achieve as high as 126 F g⁻¹. As for CB synthesized without using salt templates, only low specific capacitance (5 F g⁻¹ at 0.5 A g⁻¹) and serious loss at high rate can be obtained (Fig. S15). In addition, the electrochemical performances of HPC-BMS were also studied in a two-electrode system (Fig. S16), which is more close to the practical application. A high specific capacitance of 288 F g⁻¹ is obtained at 0.1 A g⁻¹. Meanwhile, at a high rate of 20 A g⁻¹, the HPC-BMS still maintained 175 F g⁻¹. As far as we know, such high capacitance and excellent rate performance are extremely

outstanding among similar advanced carbon-based materials (see Table 2),²⁹⁻³⁶ which should be attributed to its unique structure that endows HPC-BMS with several advantageous features. Firstly, the 3D interconnected network constructed by ultrathin carbon sheets offers effectively contact with electrolyte. More importantly, the multi-scale pores have a synergistic effect: macroporous as ion-buffering reservoirs, mesoporous channel for fully access of abundant micropores that largely enhanced surface area for charge accommodation. All these features make HPC-BMS an ideal electrode material with high specific capacitance even at ultrahigh rates. Moreover, the 3D HPC-BMS also demonstrates good cycling stability,

with approximately 91% retention of the initial specific capacitance after 10000 cycles at a current density of 5 A g⁻¹ (see Fig. 6d). As can be seen in the inset of Fig 6d, the charge/discharge curves of HPC-BMS before and after the cycling are very similar, suggesting the superb structure and chemical stability of this sample.

The electrochemical impedance spectra measurements on the electrodes of HPC-B, HPC-M, HPC-S, HPC-BM, HPC-BS, HPC-MS, and HPC-BMS after the rate capability test were also carried out to gain deeper insights into the remarkable

Table 2. The capacitive performance of advanced carbon-based materials for supercapacitors

Sample	Method	Electrolyte	Performance	Ref.
			Specific Capacitance (test condition)	
This work	Multi-template method	6M KOH	320 F g ⁻¹ (0.5 A g ⁻¹); 126 F g ⁻¹ (200 A g ⁻¹)	
Mesoporous carbon nanofibers	Solution-growth pathway	6M KOH	280 F g ⁻¹ (0.5 A g ⁻¹); 200 F g ⁻¹ (5 A g ⁻¹)	29
Porous carbon microspheres	Templated method	6M KOH	221 F g ⁻¹ (1 A g ⁻¹)	30
rGO yarn		1M H ₂ SO ₄	409 F g ⁻¹ (1 A g ⁻¹); 56 F g ⁻¹ (100 A g ⁻¹)	31
High nanoporous Carbon	Template carbonization method	6M KOH	314 F g ⁻¹ (0.5 A g ⁻¹); 95 F g ⁻¹ (100 A g ⁻¹)	32
Hierarchical carbon nanosheets	Carbonization of an organic salt	1M H ₂ SO ₄	140 F g ⁻¹ (150 A g ⁻¹)	33
3D graphene-based frameworks	Hydrothermal method	1M H ₂ SO ₄	226 F g ⁻¹ (1 mV s ⁻¹)	34
Flower-like hierarchical carbon	Hydrothermal reaction and etching	6M KOH	226 F g ⁻¹ (0.5 A g ⁻¹); 185 F g ⁻¹ (20 A g ⁻¹)	35
Hierarchical carbon	Bacteria promoted method		327 F g ⁻¹ (1 A g ⁻¹); 150 F g ⁻¹ (5 A g ⁻¹)	36

enhanced electrochemical reaction kinetics of HPC-BMS, and the results are displayed in Fig. 6e and Fig. S12f. As can be seen, all impedance spectra have similar features: a medium-to-high frequency depressed semicircle and a low-frequency linear tail, which is consistent with impedance spectra of previous carbon-based electrodes. The intercept at real part (Z') at very high frequencies represents a combined resistance of intrinsic resistance of substrate, ionic resistance of electrolyte, and contact resistance at the electrode material/current collector interface. The nearly vertical line in the low frequency region shows that the electrodes have an excellent ion diffusion

behavior. According to Fig. 6e and Fig. S12f, in the high-medium frequency region, HPC-BMS possess semicircle with smaller diameter than that of the other samples, which illustrates the HPC-BMS electrode material exhibits much lower interfacial impedance between electrolyte and electrode than the other electrode materials.

On the basis of the above results, the water-soluble salts can serve as templates to synergistically synthesize hierarchical porous carbon structure. To make this concept available for low-cost and scale-up production of 3D HPCs, abundant low-cost salts sources are highly desired. As is

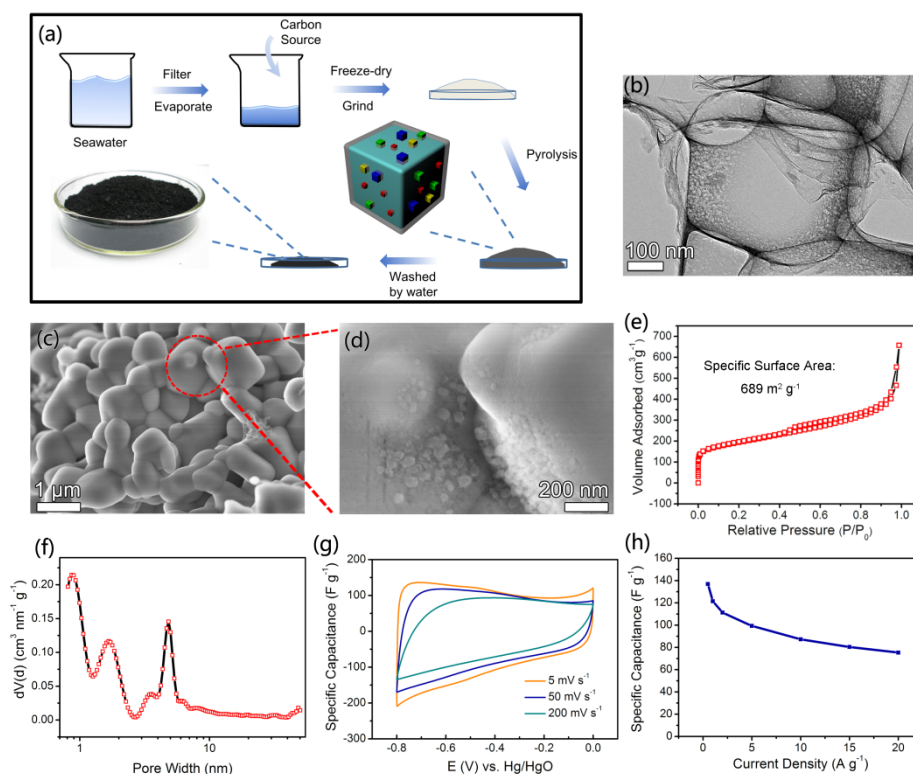


Fig. 7. (a) Schematic of fabricating hierarchical carbon structure via the assistant of seawater, and the inset is the macroscopic view of HPC-sw. (b) TEM image of HPC-sw. (c) SEM images of carbon coated sea salts before washing step. (e) Adsorption-desorption isotherms and (f) pore size distributions of HPC-sw. Electrochemical performances of HPC-sw measured in a three-electrode system: (g) CVs at different scan rates and (h) specific capacitances at different current densities.

known to all, various kinds of salt ions exist in seawater, and these ions can crystallize and act as templates for producing HPCs based on the salt self-assembly-assisted synthesis strategy. Thus, we have attempted to utilize seawater as salt template sources to produce HPCs. Fig. 7a shows the schematic of the synthesis process. In a typical experiment, the raw seawater was firstly filtered to remove the insoluble substances (such as sand and dust). Then, large part of water (~85 % of total mass) was evaporated to get seawater with high ion content, which was mixed with carbon source (glucose). After that, the mixture was subjected to the same treatment process as HPC-BMS. Finally, the carbon network with hierarchical porous structure was obtained (named as HPC-sw). SEM and TEM observations (Fig. 7 and Fig. S17) indicate that the morphology and microstructure of the as-prepared HPC-sw are very similar to that of HPC-BS, namely, the matrix is the macroporous carbon, possessing the pores with 1 μm diameter and partial regions have distribution of mesopores. During the synthesis process, NaCl served as the main template and different sources of salts emerged at the surfaces of NaCl to introduce mesopores (Fig. 7c and d). Both of High SSA ($689 \text{ m}^2 \text{ g}^{-1}$) and pore volume ($0.668 \text{ cm}^3 \text{ g}^{-1}$) suggest that HPC-sw is a promising candidate as electrode of supercapacitor (Fig. 7e and f), which shows rectangular shape of CV curves (Fig. 8g) at different scan rates ($5\text{--}200 \text{ mV s}^{-1}$). At a current density of 0.5 A g^{-1} , the calculated capacitance is up to 125 F g^{-1} (Fig. 7h). While the specific capacitance still keeps at 84 F g^{-1} at a high current density of 20 A g^{-1} .

Conclusions

In summary, we have reported a novel, simple and scalable approach to produce 3D interconnected hierarchical porous carbon using the self-assembly of various water-soluble NaX salts ($X: \text{Cl}^-, \text{CO}_3^{2-}, \text{SiO}_3^{2-}$) as a structure-directing template. By controlling crystallization and assembly of multi-scale salts via freeze-drying processing, 3D porous carbon networks with tailored pore size distribution have been achieved by calcining the salts/glucose self-assembly followed by removing the 3D self-assembly of NaX salts via simple water washing. A typical 3D HPCs produced with the assistance of self-assembly template of NaCl, Na_2CO_3 and Na_2SiO_3 is capable of delivering a high specific capacitance of 320 F g^{-1} at a current density of 0.5 A g^{-1} and retained ~40% capacitance at 200 A g^{-1} . In addition, no apparent discharge capacity decay between 1000 and 10 000 continuous charge-discharge cycles is observed at a high current density of 5 A g^{-1} , indicating the excellent specific capacitance retention ability. The excellent performance is attributed to the 3D hierarchical porous network structure with broad ion diffusion pathway, low charge-transfer resistance, and robust structure at high current density for long-time cycling. Based on our soluble salt self-assembly-assisted synthesis concept, it was revealed that salts in the seawater are also very suitable for low-cost and scalable synthesis of 3D HPCs with good capacitive performance, which pave the way for advanced utilization of seawater.

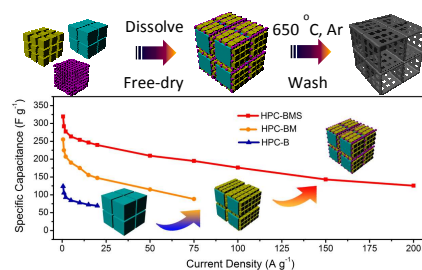
Acknowledgements

This work was supported by the National Natural Science Foundation of China No.51422104, No. 51272173 and No. 51472177, China-EU Science and Technology Cooperation Project (No. 1206)

Notes and references

- 1 Y. Zhu, S. Murali, M. D. Stoller, K. Ganesh, W. Cai, P. J. Ferreira, A. Pirkle, R. M. Wallace, K. A. Cychoz, M. Thommes, *Science*, 2011, **332**, 1537-1541.
- 2 F. W. Richey, B. Dyatkin, Y. Gogotsi, Y. A. Elabd, *J. Am. Chem. Soc.*, 2013, **135**, 12818-12826.
- 3 B. G. Choi, M. Yang, W. H. Hong, J. W. Choi, Y. S. Huh, *ACS Nano*, 2012, **6**, 4020-4028.
- 4 H. Jiang, P. S. Lee, C. Li, *Energy Environ. Sci.*, 2013, **6**, 41-53.
- 5 J. Wei, D. Zhou, Z. Sun, Y. Deng, Y. Xia, D. Zhao, *Adv. Funct. Mater.*, 2013, **23**, 2322-2328.
- 6 S. L. Candelaria, Y. Shao, W. Zhou, X. Li, J. Xiao, J.-G. Zhang, Y. Wang, J. Liu, J. Li, G. Cao, *Nano Energy*, 2012, **1**, 195-220.
- 7 H. Wang, H. Dai, *Chem. Soc. Rev.*, 2013, **42**, 3088-3113.
- 8 N. D. Petkovich, A. Stein, *Chem. Soc. Rev.*, 2013, **42**, 3721-3739.
- 9 Y. Fang, Y. Lv, R. Che, H. Wu, X. Zhang, D. Gu, G. Zheng, D. Zhao, *J. Am. Chem. Soc.*, 2013, **135**, 1524-1530.
- 10 J. Lee, J. Kim, T. Hyeon, *Adv. Mater.*, 2006, **18**, 2073-2094.
- 11 N. P. Stadie, M. Murialdo, C. C. Ahn, B. Fultz, *J. Am. Chem. Soc.*, 2013, **135**, 990-993.
- 12 A. Vu, X. Li, J. Phillips, A. Han, W. H. Smyrl, P. Bühlmann, A. Stein, *Chem. Mater.*, 2013, **25**, 4137-4148.
- 13 J.-S. Yu, S. Kang, S. B. Yoon, G. Chai, *J. Am. Chem. Soc.*, 2002, **124**, 9382-9383.
- 14 X. Y. Chen, Y. Y. He, H. Song, Z. J. Zhang, *Carbon*, 2014, **72**, 410-420.
- 15 A. B. Fuertes, M. Sevilla, *ACS Appl. Mater. Inter.*, 2015, **7**, 4344-4353.
- 16 Z. S. Wu, Y. Sun, Y. Z. Tan, S. B. Yang, X. L. Feng, K. Mullen, *J. Am. Chem. Soc.*, 2012, **134**, 19532-19535.
- 17 J. Y. Liang, S. L. Chen, M. J. Xie, Y. Z. Wang, X. K. Guo, X. F. Guo, W. P. Ding, *J. Mater. Chem. A*, 2014, **2**, 16884-16891.
- 18 H. Jiang, P. S. Lee, C. Li, *Energy Environ. Sci.*, 2013, **6**, 41-53.
- 19 Y. Zeng, K. Wang, J. Yao, H. Wang, *Carbon*, 2014, **69**, 25-31.
- 20 W. Kwon, G. Lee, S. Do, T. Joo, S. W. Rhee, *Small*, 2014, **10**, 506-513.
- 21 C. M. Ghimbeu, L. Vidal, L. Delmotte, J.-M. Le Meins, C. Vix-Guterl, *Green Chem.*, 2014, **16**, 3079-3088.
- 22 A. D. Roberts, X. Li, H. Zhang, *Chem. Soc. Rev.*, 2014, **43**, 4341-4356.
- 23 S. Zhang, L. Chen, S. Zhou, D. Zhao, L. Wu, *Chem. Mater.*, 2010, **22**, 3433-3440.
- 24 S. B. Yoon, K. Sohn, J.Y. Kim, J.-S. Yu, T. Hyeon, *Adv. Mater.*, 2002, **14** 19-21.
- 25 N. Fechler, T. Fellingner, M. Antonietti, *Adv. Mater.*, 2013, **25**, 75-79.
- 26 J. Zhou, J. Qin, X. Zhang, C. Shi, E. Liu, J. Li, N. Zhao, C. He *ACS Nano*, 2015, **9**, 3837-3848.
- 27 P. Yang, W. Mai, *Nano Energy*, 2014, **8**, 274-290.
- 28 X. Li, B. Wei, *Nano Energy*, 2013, **2**, 159-173.
- 29 J. Qin, C. He, N. Zhao, Z. Wang, C. Shi, E.-Z. Liu, J. Li, *ACS Nano*, 2014, **8**, 1728-1738.
- 30 L. Chen, Z. Wang, C. He, N. Zhao, C. Shi, E. Liu, J. Li, *ACS Appl. Mater. Inter.*, 2013, **5**, 9537-9545.
- 31 L.-F. Chen, X.-D. Zhang, H.-W. Liang, M. Kong, Q.-F. Guan, P. Chen, Z.-Y. Wu, S.-H. Yu, *ACS Nano*, 2012, **6**, 7092-7102.
- 32 J. Chmiola, C. Largeot, P.-L. Taberna, P. Simon, Y. Gogotsi, *Science*, 2010, **328**, 480-483.
- 33 S. Chen, W. Xing, J. Duan, X. Hu, S. Z. Qiao, *J. Mater. Chem. A*, 2013, **1**, 2941-2954.
- 34 W. Li, F. Zhang, Y. Dou, Z. Wu, H. Liu, X. Qian, D. Gu, Y. Xia, B. Tu, D. Zhao, *Adv. Energy Mater.*, 2011, **1**, 382-386.
- 35 Q. L. Zhao, X. Y. Wang, C. Wu, J. Liu, H. Wang, J. Gao, Y. W. Zhang, H. B. Shu, *J. Power Sources*, 2014, **254**, 10-17.
- 36 S. H. Aboutalebi, R. Jalili, D. Esrafilzadeh, M. Salari, Z. Gholamvand, S. Yamini, K. Konstantinov, R. L. Shepherd, J. Chen, S. Moulton, *ACS Nano*, 2014, **8**, 2456-2466.

Graphical abstract



Three-dimensional hierarchical porous carbons are synthesized via a simple one-pot method using the self-assembly of various water-soluble salts as a structure-directing template, which exhibit excellent capacitive performance.